JOURNAL OF BACTERIOLOGY, May 2006, p. 3498–3506 Vol. 188, No. 10
0021-9193/06/$08.00+0 doi:10.1128/JB.188.10.3498–3506.2006

WrbA from *Escherichia coli* and *Archaeoglobus fulgidus* Is an NAD(P)H:Quinone Oxidoreductase

Eric V. Patridge and James G. Ferry*

Department of Biochemistry and Molecular Biology, Eberly College of Science, The Pennsylvania State University, 205 South Frear Laboratory, University Park, Pennsylvania 16802-4500

Received 19 December 2005/Accepted 6 March 2006

WrbA (tryptophan [W] repressor-binding protein) was discovered in *Escherichia coli*, where it was proposed to play a role in regulation of the tryptophan operon; however, this has been put in question, leaving the function unknown. Here we report a phylogenetic analysis of 30 sequences which indicated that WrbA is the prototype of a distinct family of flavoproteins which exists in a diversity of cell types across all three domains of life and includes documented NAD(P)H:quinone oxidoreductases (NQOs) from the *Fungi* and *Viridiplantae* kingdoms. Biochemical characterization of the prototypic WrbA protein from *E. coli* and WrbA from *Archaeoglobus fulgidus*, a hyperthermophilic species from the *Archaea* domain, shows that these enzymes have NQO activity, suggesting that this activity is a defining characteristic of the WrbA family that we designate a new type of NQO (type IV). For *E. coli* WrbA, the K_m^{NADH} was 14 ± 0.43 μM and the $K_m^{benzoquinone}$ was 5.8 ± 0.12 μM. For *A. fulgidus* WrbA, the K_m^{NADH} was 19 ± 1.7 μM and the $K_m^{benzoquinone}$ was 37 ± 3.6 μM. Both enzymes were found to be homodimeric by gel filtration chromatography and homotetrameric by dynamic light scattering and to contain one flavin mononucleotide molecule per monomer. The NQO activity of each enzyme is retained over a broad pH range, and apparent initial velocities indicate that maximal activities are comparable to the optimum growth temperature for the respective organisms. The results are discussed and implicate WrbA in the two-electron reduction of quinones, protecting against oxidative stress.

The tryptophan (W) repressor-binding protein (WrbA) from *Escherichia coli* ($WrbA_{E.\ coli}$) was discovered in 1993, when it was copurified with the tryptophan repressor (TrpR) (66). Biochemical characterization of $WrbA_{E.\ coli}$ showed that the protein binds one flavin mononucleotide (FMN) molecule per monomer and is multimeric in solution (29). These results, combined with sequence analysis and homology-based structural modeling, led to the suggestion that $WrbA_{E.\ coli}$ is the founding member of a new family of multimeric flavodoxin-like proteins. It was predicted that the WrbA family contains an αβ twisted open-sheet fold characteristic of flavodoxins and a conserved insertion after strand β4, forming an additional αβ unit (28). The presence of this fold has recently been confirmed in the published crystal structures of the *Deinococcus radiodurans* and *Pseudomonas aeruginosa* WrbA homologues (26). $WrbA_{E.\ coli}$ is the only purified and biochemically characterized WrbA protein in the literature. No enzyme activity was reported; however, it was reported that $WrbA_{E.\ coli}$ enhances the development of noncovalent complexes between the TrpR holorepressor and operator DNA and that $WrbA_{E.\ coli}$ alone is not competent to interact with the DNA targets (66). Thus, it was proposed that $WrbA_{E.\ coli}$ is an accessory element which blocks TrpR-specific transcriptional events that are deleterious to cells entering stationary phase. However, it was later concluded that $WrbA_{E.\ coli}$ does not specifically affect the TrpR-DNA complex, placing the earlier proposed function in doubt (29). Thus, the function of WrbA is unknown.

* Corresponding author. Mailing address: Department of Biochemistry and Molecular Biology, Eberly College of Science, The Pennsylvania State University, 205 South Frear Laboratory, University Park, PA 16802-4500. Phone: (814) 863-5721. Fax: (814) 863-6217. E-mail: jgf3@psu.edu.

Several global expression studies show that *wrbA* in *E. coli* is under the control of RpoS (the stress response sigma factor, σ^s or σ^{38}). These studies report that *wrbA* is upregulated in response to stressors such as acids, salts, H_2O_2, and diauxie. $WrbA_{E.\ coli}$ is also upregulated in the early stages of the stationary phase, indicating that it could play a role in preparing the cell for long-term maintenance under stress conditions (14, 17, 31, 35, 50, 51, 59, 61). Two additional expression studies implicate $WrbA_{E.\ coli}$ in oxidative stress. One study shows that *E. coli wrbA* is repressed when ArcA is phosphorylated, which occurs when the quinone pool is reduced (41), and another study shows that *E. coli wrbA* is repressed by fumarate and nitrate reductase regulatory protein under anaerobic conditions (34). Aside from these findings, nothing is known about the role of WrbA in the stress response.

The most comprehensive sequence analysis of $WrbA_{E.\ coli}$ was reported in 1994 by Grandori and Carey (28). Since that time, genomic sequencing has identified more than 100 genes annotated as encoding WrbA from metabolically and phylogenetically diverse prokaryotes spanning the *Bacteria* and *Archaea* domains, consistent with a fundamental function for the WrbA family in the physiology of prokaryotes. However, $WrbA_{E.\ coli}$ is the only WrbA that has been biochemically characterized. Here we show that several biochemically characterized NAD(P)H:quinone oxidoreductases (NQOs) from the *Fungi* and *Viridiplantae* kingdoms have significant sequence identity to WrbA and belong to the same family (10, 11, 18, 33, 37, 44, 64). We also report the initial biochemical characterization of WrbA from *Archaeoglobus fulgidus* ($WrbA_{A.\ fulgidus}$), a hyperthermophile and a representative of the *Archaea* domain, and demonstrate that $WrbA_{E.\ coli}$ and $WrbA_{A.\ fulgidus}$ exhibit robust NQO activity. The results presented are consistent with a role for WrbA

in the oxidative stress response of diverse prokaryotes from the *Bacteria* and *Archaea* domains.

MATERIALS AND METHODS

Materials and reagents. Primers were obtained through Integrated DNA Technologies (Coralville, IA). *E. coli* K-12 MG1655 genomic DNA was a gift from Sue-Jean Hong and Kenneth Keiler (The Pennsylvania State University). All materials used to construct *E. coli* knockouts were gifts from Joe Palladino and Sarah Ades (The Pennsylvania State University). *A. fulgidus* genomic DNA was a gift from Michael W. Adams (University of Georgia). All cell lines and plasmids were obtained through Novagen (Madison, WI). The chromatography resins and equipment were purchased from Amersham Biosciences, (Piscataway, NJ). F_{420} and 2-hydroxyphenazine were gifts from Uwe Deppenmeier. All other chemicals were purchased from ICN (MP Biomedical), Sigma, or ACROS. Phenotypic analysis of the *E. coli wrbA* mutant strain was contracted to Phenotype MicroArray Services at Biolog, Inc. (Hayward, CA).

Sequence alignments and construction of the phylogenetic tree. Sequences were aligned with ClustalX (v1.83) with a BLOSUM62 matrix and default parameters. The output was edited with the Alignment Editor of MEGA (v3.1) and visualized with BioEdit (v7.0.5.2). The phylogenetic tree was constructed with the MEGA package. Distance matrices were generated in MEGA by the minimum-evolution method with the Jones-Taylor-Thornton option and the close-neighbor interchange option with a search level of 1. Gaps were deleted in a pairwise manner. The confidence limits of the nodes were estimated with the bootstrap option. Phylogenetic trees were also constructed by the parsimony method, the neighbor-joining method, and the unweighted-pair group method using average linkages available in MEGA, but the minimum-evolution method produced the tree with the greatest bootstrap values.

Cloning, expression, purification, and reconstitution. The b1004 open reading frame (ORF) was amplified by PCR from *E. coli* K-12 MG1655 genomic DNA with sense (ATGGCTAAAGTTCTGGTGC) and antisense (CCTCCTGTTGA AGATTAGCC) primers. The AF0343 ORF was amplified by PCR from *A. fulgidus* genomic DNA with sense (ATGGCCAGGATTCTTGTTATTTTTCA TTCC) and antisense (CCCTTAGCAGAGCTTTTCAGCCACCTC) primers. Each PCR product was amplified and cloned into pETBlue-1 to obtain recombinant plasmids pETecb1004 from b1004 and pETaf0343 from AF0343. *E. coli* NovaBlue cells were used to amplify each plasmid. DNA sequencing confirmed that *E. coli wrbA* and *A. fulgidus wrbA* were intact in pETecb1004 and pETaf0343, respectively. Since the AF0343 ORF contains 12% rare codons with two rare-codon repeats, pETecb1004 and pETaf0343 were each transformed into *E. coli* RosettaBlue(DE3)pLacI competent cells for expression. The transformed cells were cultured at 37°C in terrific broth containing 50 μg/ml ampicillin and 34 μg/ml chloramphenicol. When the optical density at 600 nm reached 0.6, production of $WrbA_{E.\ coli}$ or $WrbA_{A.\ fulgidus}$ was induced by the addition of 0.4 mM isopropyl-β-D-thiogalactopyranoside (IPTG) at 37°C. Cells were harvested after 4 h by centrifugation and stored at −80°C.

Initial purification and reconstitution of $WrbA_{A.\ fulgidus}$ were carried out anaerobically with an anaerobic chamber (COY Laboratory Products, Ann Arbor, MI) and at room temperature except where indicated otherwise. A comparison of the aerobic and anaerobic protocols showed no difference in the measured activities of purified protein; thus, all subsequent purifications were carried out aerobically. For $WrbA_{A.\ fulgidus}$, thawed cells (10 g [wet weight]) were resuspended in 45 ml of 50 mM sodium phosphate buffer (pH 6.6) and lysed by three passes through a French press at 20,000 lb/in^2 (137.9 MPa). Cell debris was removed by centrifugation at 65,000 × *g* for 45 min at 4°C, and the cleared lysate was diluted to 80 ml with 50 mM sodium phosphate buffer (pH 6.6) and incubated at 75°C for 30 min while stirring. Denatured proteins were pelleted by centrifugation at 65,000 × *g* for 45 min at 4°C. The supernatant was filtered and loaded onto a Q-Sepharose column equilibrated with 50 mM sodium phosphate buffer (pH 6.6). The column was developed with a 0.0 to 0.4 M NaCl linear gradient over 500 ml, applied at 2 ml/min. Yellow fractions containing $WrbA_{A.\ fulgidus}$, monitored by sodium dodecyl sulfate-polyacrylamide gel electrophoresis (SDS-PAGE), were pooled, diluted fourfold with 50 mM sodium phosphate buffer (pH 7.8), and loaded onto a Q-Sepharose column equilibrated with 50 mM sodium phosphate buffer (pH 7.8). The column was developed with a 0.0 to 0.4 M NaCl linear gradient over 500 ml, applied at 2 ml/min. Yellow fractions containing $WrbA_{A.\ fulgidus}$, monitored by SDS-PAGE, were pooled and concentrated to 1 ml with a Vivacell 70 with a 10,000 molecular weight cutoff membrane (Vivascience, Hanover, Germany). The concentrated solution was loaded onto a Sephadex-200 column equilibrated with 150 mM morpholinepropanesulfonic acid (MOPS; pH 7.2). Yellow fractions containing-$WrbA_{A.\ fulgidus}$, monitored by SDS-PAGE, were pooled and incubated with 5 mM FMN for 16 h at 4°C. This solution was then dialyzed against 50 mM MOPS (pH 7.2) and concentrated to 2.5 ml. Excess FMN was removed by passage through a PD-10 column, and the solution containing FMN-reconstituted $WrbA_{A.\ fulgidus}$ was stored at −80°C.

The same protocol was used for the purification and reconstitution of $WrbA_{E.\ coli}$, except that heat denaturation was excluded from the protocol.

Biochemical analyses. The subunit molecular mass of each protein was estimated by 12% SDS-PAGE with low-molecular-weight markers from Bio-Rad. Native molecular mass was estimated from the elution volume from a Sephadex-S200 gel filtration fast protein liquid chromatography column calibrated with the following proteins of known molecular masses: bovine serum albumin (66 kDa), ovalbumin (45 kDa), carbonic anhydrase (31 kDa), chymotrypsinogen (25 kDa), and RNase A (13.7 kDa). The buffer (50 mM MOPS, 150 mM NaCl, pH 7.2) was applied at 0.5 ml min^{-1}. Further oligomerization was estimated by dynamic light-scattering analyses, which were performed in triplicate with each analysis incorporating at least 10 readings.

After reconstitution, the Pierce assay was used to determine protein concentrations. Flavin/monomer ratios were calculated after quantifying the amount of FMN released by acidification (5% trichloroacetic acid) with an extinction coefficient for FMN of 12.2 mM^{-1} cm^{-1} at 450 nm.

The flavin cofactor of $WrbA_{E.\ coli}$ was previously identified as FMN (29). To identify the flavin in $WrbA_{A.\ fulgidus}$, the flavin cofactor was extracted from purified protein by acidification of the protein solution with 5% trichloroacetic acid. A Hewlett-Packard model 1050 high-performance liquid chromatography system in conjunction with a Hewlett-Packard LiChrosorb C_{18} reversed-phase column was used to identify the flavin extracted from $WrbA_{A.\ fulgidus}$. Neutralized samples were injected into a mobile phase consisting of 10 mM potassium phosphate, 12.5% acetonitrile, 0.3% triethylamine, and 0.01% sodium azide at a pH of 6.5. Elution of flavin was monitored at 450 nm.

Activities. Reactions were monitored with a Varian Cary 50 spectrophotometer in combination with a Peltier thermostat-equipped accessory and an anaerobic fluorescence cuvette (2 mm by 1 cm [path length]) from Starna (Atascadero, CA). Although fluorescence was not measured, the cuvette permitted small reaction volumes under anaerobic conditions, and the 2-mm path length permitted high concentrations of NADH to be accurately determined spectroscopically. $WrbA_{A.\ fulgidus}$ activity measurements were obtained at 65°C, and $WrbA_{E.\ coli}$ activity measurements were obtained at 37°C unless indicated otherwise. Reactions were initiated by addition of the enzyme after temperature equilibration of the assay mixture. All activities were performed in triplicate, and all nonenzymatic rates were taken into account.

NADH was used as the electron donor to determine the specific activities of $WrbA_{E.\ coli}$ and $WrbA_{A.\ fulgidus}$ with a variety of electron acceptors. Reaction mixtures contained 50 mM MOPS (pH 7.2) with 800 μM NADH, 400 μM electron acceptor, and variable concentrations of $WrbA_{E.\ coli}$ or $WrbA_{A.\ fulgidus}$. With 1,4-benzoquinone and 2,3-dihydroxy-5-methyl-1,4-benzoquinone, oxidation of NADH was monitored at 340 nm (ε_{340} = 6.22 mM^{-1} cm^{-1}). With menadione, NADH oxidation was monitored at 341 nm (ε_{341} = 6.22 mM^{-1} cm^{-1}), which is the isosbestic point for menadione at both 37°C and 65°C. With naphthoquinone, oxidation was measured at the appropriate isosbestic point of naphthoquinone, which shifted from 340 nm at 37°C to 341 nm at 65°C. With K_3FeCN_6 (ε_{420} = 1.04 mM^{-1} cm^{-1}) and 2,6-dichlorophenolindophenol (ε_{610} = 21 mM^{-1} cm^{-1}), the rates of reduction were monitored at the indicated wavelengths. The initial 10 s of each progress curve was taken as the apparent initial velocity. Nonenzymatic reactions represented <8% of all enzymatic reaction conditions.

Steady-state kinetic studies were conducted with 50 mM MOPS (pH 7.2) at 37°C and various enzyme concentrations. The kinetic parameters for 1,4-benzoquinone were determined by monitoring the oxidation of 200 μM NADH at 340 nm. The kinetic parameters for NAD(P)H were determined by monitoring the reduction of 200 μM K_3FeCN_6 at 420 nm. Benzoquinone and NAD(P)H concentrations were varied from 0.2 to 10 times the respective K_m values. The initial 2 to 5 s of each progress curve was taken as the apparent initial velocity, and the Michaelis-Menten equation was fitted to the data with KaleidaGraph v3.5. Nonenzymatic reactions represented <2% of all enzymatic reaction conditions.

The pH dependence of apparent initial velocities for electron transfer from NADH to menadione was measured over a wide pH range by monitoring the oxidation of NADH at 341 nm. Reaction mixtures contained 800 μM NADH, 400 μM menadione, and 0.1 μM $WrbA_{E.\ coli}$ or 0.03 μM $WrbA_{A.\ fulgidus}$. For $WrbA_{E.\ coli}$, a buffer mixture with 50 mM each Na-acetate–morpholineethanesulfonic acid (MES)–MOPS–Tris(hydroxymethyl)methylaminopropanesulfonic acid, sodium salt (TAPS) was used from pH 4.0 to 8.5. This buffer mixture was also used for $WrbA_{A.\ fulgidus}$ from pH 4.0 to 8.0, and a second buffer mixture (50 mM TAPS, 50 mM glycine) was used from pH 7.5 to 9.5. The initial 10 s of each progress curve was taken as the apparent initial velocity. Nonenzymatic reactions represented <8% of all enzymatic reaction conditions.

The temperature dependence of apparent initial velocities for electron transfer from NADH to menadione was determined by monitoring the oxidation of NADH at 341 nm. Reaction mixtures contained 800 μM NADH, 400 μM menadione, and 0.1 μM $WrbA_{E.\ coli}$ or 0.03 μM $WrbA_{A.\ fulgidus}$. All reactions were performed in 50 mM sodium phosphate (pH 7.2) at 25°C. $WrbA_{E.\ coli}$ was assayed from 10°C to 60°C, and $WrbA_{A.\ fulgidus}$ was assayed from 10°C to 100°C. The initial 5 s of each progress curve was taken as the apparent initial velocity. Nonenzymatic reactions represented <8% of all enzymatic reaction conditions.

Disruption of *wrbA*. *E. coli* K-12 MG1655 (F^- lambda$^-$ *ilvG rfb-50 rph-1*) was used as the wild-type (WT) strain, and disruption of *wrbA* was conducted according to previously published methods (20). Primers were constructed with the pKD4 template, and kanamycin resistance genes were eliminated by with the pCP20FLP helper plasmid. Elimination of temperature-sensitive plasmids and thermal induction of the FLP recombinase synthesis were carried out with Luria broth at 43°C.

RESULTS

Homology, sequence analysis, and phylogeny. The most comprehensive sequence analysis of $WrbA_{E.\ coli}$, the only biochemically characterized WrbA to date, was done in 1994, when $WrbA_{E.\ coli}$ was suggested to be the prototype of a new family of flavoproteins (28). However, the analysis included only six sequences of putative WrbA homologues; therefore, a BLAST search of all nonredundant databases was performed with the 198-residue protein sequence of $WrbA_{E.\ coli}$, encoded by locus b1004 in *E. coli* K-12 MG1655, as the query. A survey of the returned 394 sequences revealed 128 predicted WrbA proteins that had between 22% and 99% identity to $WrbA_{E.\ coli}$.

The genes neighboring the loci encoding the WrbA homologues were surveyed, but no consistencies were found to suggest a common function. The returned BLAST results included 20 sequences annotated as fungal and plant quinone reductases, suggesting that these enzymes could be related to WrbA. Among the aligned data set were five documented NQOs from the *Fungi* and *Viridiplantae* kingdoms that are biochemically characterized (FQR1 from *Arabidopsis thaliana*, QR1 and QR2 from *Gloeophyllum trabeum*, QR from *Phanerochaete chrysosporium*, and QR2 from *Triphysaria versicolor*) (10, 11, 18, 33, 37, 44). These five documented quinone reductases have between 43% and 48% identity to $WrbA_{E.\ coli}$. Replicate sequences, truncated sequences, and sequences with partial alignments were removed from the BLAST results, and an initial phylogenetic tree was constructed with an alignment of the remaining 208 sequences (not shown). From the collected sequences, 30 were selected to represent the initial tree. These sequences were aligned (Fig. 1), and a bootstrapped phylogenetic tree was constructed by the minimum-evolution method with three flavodoxin sequences to root the tree (Fig. 2). The clustering of the initial phylogenetic tree indicated that all of the proteins included in the data set diverged from a common ancestor distinct from classical flavodoxins. Moreover, these results identify NQOs as members of the WrbA family. The tree contained a diverse set of organisms from all three domains of life, which included psychrophiles, mesophiles, thermophiles, animal and plant pathogens, aerobes, and anaerobes. The tree also contained 8 NQO sequences from the *Fungi* and *Viridiplantae* kingdoms and 15 and 6 WrbA sequences from the *Bacteria* and *Archaea* domains, respectively.

The PROSITE flavodoxin signature sequence (LIV)(LIVFY)(FY)X(ST)(V)X(AGC)XT(P)XXAXX(LIV), indicative of the N-terminal region that spans an FMN-binding site, was present across all aligned sequences, with little deviation from the motif (Fig. 1). The αβ twisted open-sheet fold typical of flavodoxins is present across all sequences of the aligned data set, with an additional αβ unit previously reported for the WrbA family (28). The invariant conservation of this additional αβ unit (Fig. 1) further supports the idea that the NQO and WrbA proteins diverged from a common ancestor distinct from classical flavodoxins. These results solidify the earlier proposal (28) of a new family of flavoproteins and further extends the WrbA family to all three domains of life.

In surveying the BLAST results, it was discovered that several sequences annotated as WrbA contain a motif strictly conserved in another FMN-containing protein family called iron-sulfur flavoprotein (Isf) (2, 5, 38, 39, 67). However, the Isf family contains an unusual compact cysteine motif ($CX_2CX_2CX_{5-7}C$) that binds a 4Fe-4S cluster not found in the sequences of WrbA proteins or the NQO enzymes aforementioned. A sequence alignment was constructed to address the relatedness between the Isf and WrbA families. The alignment included $WrbA_{E.\ coli}$ and $WrbA_{A.\ fulgidus}$, representing the WrbA family; three Isf sequences, including the prototype (Isf from *Methanosarcina thermophila*); and seven misannotated WrbA sequences that contained the compact cysteine motif. Flavodoxin 5NLL from *Clostridium beijerinckii* was included for comparison to characterized flavodoxins (Fig. 3). The alignment demonstrates that the misannotated WrbA sequences with the compact cysteine motif belong to the Isf family. While Fig. 3 indicates that similarity persists across the alignment, the overall identity between WrbA and Isf sequences suggests significant deviation from a common ancestor. In deviating from the common ancestor, it is possible that either Isf lost the domain containing the 4Fe-4S cluster-binding motif, giving rise to the WrbA family, or WrbA acquired the domain, giving rise to the Isf family.

Biochemical characterization of $WrbA_{E.\ coli}$ and $WrbA_{A.\ fulgidus}$. $WrbA_{E.\ coli}$ is the only prokaryotic WrbA biochemically characterized; thus, $WrbA_{A.\ fulgidus}$ from the *Archaea* domain was heterologously produced in *E. coli* and characterized for comparison to $WrbA_{E.\ coli}$ from the *Bacteria* domain. $WrbA_{E.\ coli}$ has 43% identity and 62% similarity to $WrbA_{A.\ fulgidus}$, encoded by locus AF0343 in *A. fulgidus*. $WrbA_{E.\ coli}$ and $WrbA_{A.\ fulgidus}$ were each overexpressed in *E. coli* and purified to homogeneity, as determined by SDS-PAGE. The identity of each protein was confirmed by N-terminal sequencing of the first five residues: AKVLV for $WrbA_{E.\ coli}$ and ARILV for $WrbA_{A.\ fulgidus}$. SDS-PAGE revealed that the subunit molecular mass of $WrbA_{A.\ fulgidus}$ was 22.1 kDa and that of $WrbA_{E.\ coli}$ was 21.2 kDa. Size exclusion chromatography showed that $WrbA_{A.\ fulgidus}$ had a native molecular mass of 52 kDa, suggesting that $WrbA_{A.\ fulgidus}$ is able to form a dimer, as previously reported for $WrbA_{E.\ coli}$ (29). Dynamic light-scattering analyses support the idea that both $WrbA_{E.\ coli}$ and $WrbA_{A.\ fulgidus}$ participate in tetramerization. Purified $WrbA_{E.\ coli}$ had a hydrodynamic radius of 3.9 ± 0.12 nm, corresponding to a molecular mass of 79 ± 6.7 kDa, while purified $WrbA_{A.\ fulgidus}$ had a hydrodynamic radius of 4.1 ± 0.12 nm, corresponding to a molecular mass of 89 ± 8.4 kDa. Each sample was found to be monodisperse, with $WrbA_{E.\ coli}$ or $WrbA_{A.\ fulgidus}$ representing over 99.5% of the mass. During purification, $WrbA_{E.\ coli}$ retained FMN during elution from the first Q-Sepharose column

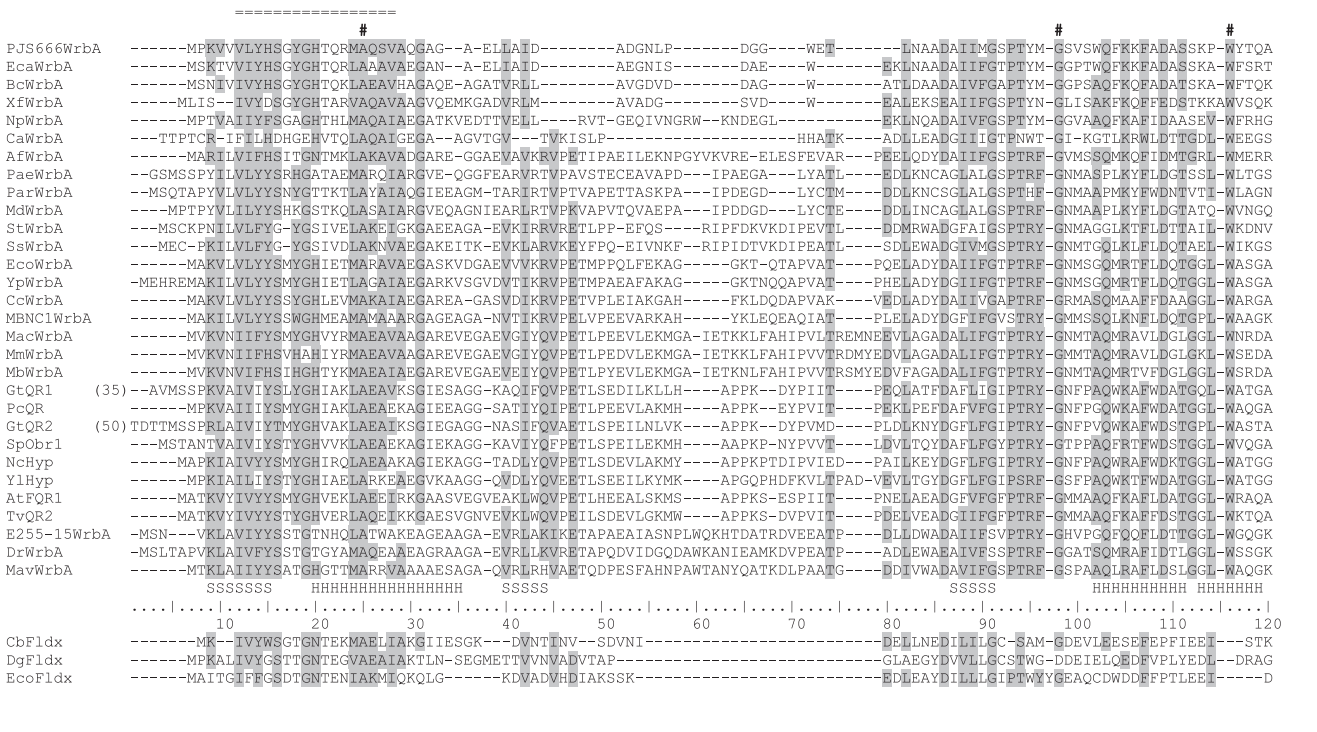

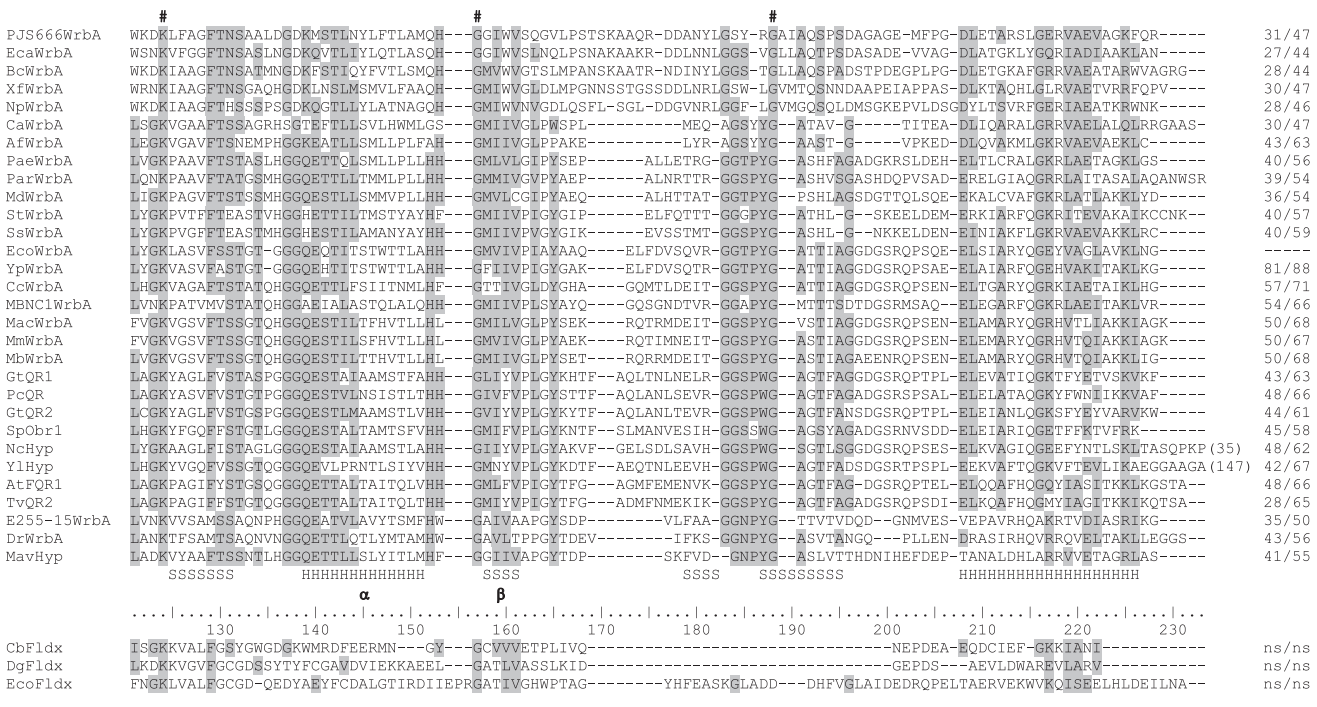

FIG. 1. Alignment of WrbA, NAD(P)H:quinone oxidoreductase, and flavodoxin sequences. Numerical values at the C terminus indicate percent identity/percent similarity to WrbA$_{E.\ coli}$. ns, not significant; #, completely conserved residue. Shaded residues indicate that a conservation of similar residues persists across at least 60% of the alignment. = = = = = = = =, region of the flavodoxin signature motif. JPred at ExPASy's Proteomic Tools was used to predict α-helix (HHHH) and β-sheet (SSSS) sequences with the alignment (flavodoxin sequences were excluded). The additional αβ unit that is discussed is indicated in bold below the secondary-structure prediction. Organisms and ORF designations from the corresponding genomic sequence: *A. fulgidus* WrbA (gi: 11497955), *A. thaliana* FQR1 (gi: 21539481), *Burkholderia cepacia* WrbA (gi: 46310790), *Chloroflexus aurantiacus* WrbA (gi: 53798190), *Caulobacter crescentus* WrbA (gi: 13422034), *C. beijerinckii* Fldx (gi: 1941945), *Desulfovibrio gigas* Fldx (gi: 40801), *D. radiodurans* WrbA (gi: 58177611), *Exiguobacterium* sp. strain 255-15 WrbA (gi: 68054352), *Erwinia carotovora* WrbA (gi: 49613050), *E. coli* WrbA (gi: 148264), *G. trabeum* QR1 (gi: 30027749) and QR2 (gi: 33668045), *Methanosarcina acetivorans* WrbA (gi: 19915027), *Mycobacterium avium* WrbA (gi: 41409133), *Methanosarcina barkeri* WrbA (gi: 31793946) and Fldx (gi: 72396729), *Mezorhizobium* sp. strain BNC1 WrbA (gi: 68191386), *Microbulbifer degredans* WrbA (gi: 48860599), *Methanosarcina mazei* WrbA (gi: 21228326), *Neurospora crassa* Hyp (gi: 38566940), *Nostoc punctiforme* WrbA (gi: 23129682), *Psychrobacter arcticum* WrbA(gi: 71038102), *P. chrysosporium* QR (gi: 4454993), *Polaromonas* sp. strain JS666 WrbA (gi: 67847813), *P. aeruginosa* WrbA (gi: 9946855), *S. pombe* Obr1 (gi: 2462689), *Sulfolobus solfataricus* WrbA (gi: 15899861), *Sulfolobus todakii* WrbA (gi: 15621890), *T. versicolor* QR2 (gi: 12484052), *Xylella fastidiosa* WrbA (gi: 22993897), *Yarrowia lipolytica* Hyp (gi: 49647887), and *Yersinia pestis* WrbA (gi: 22126332).

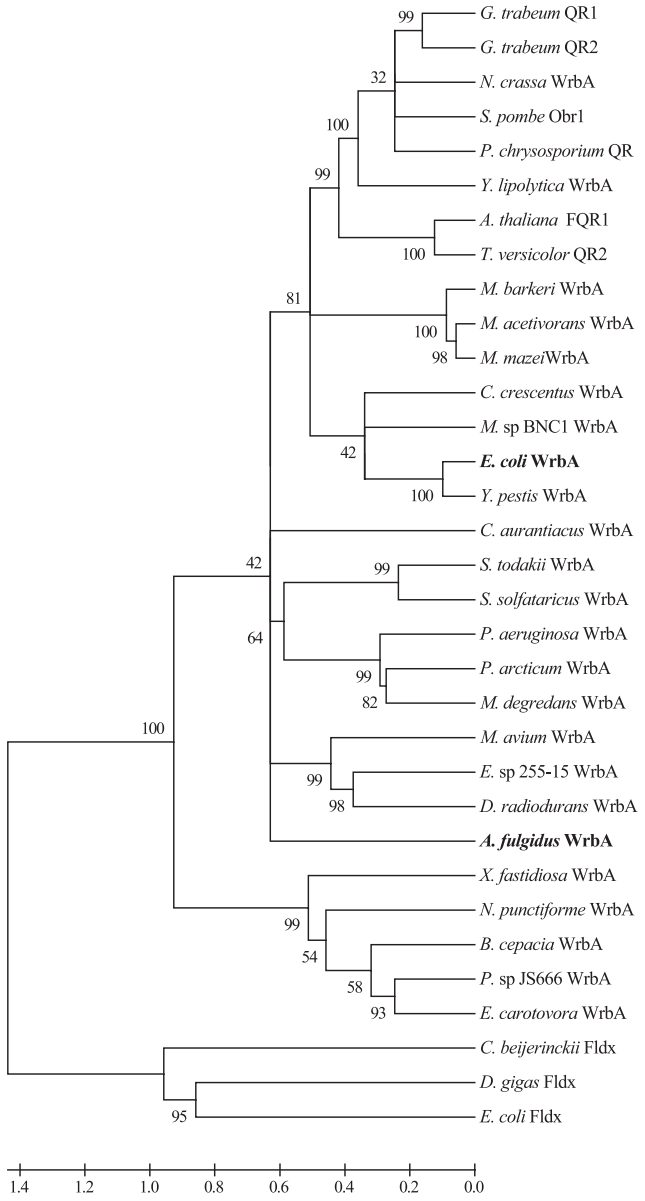

FIG. 2. Phylogenetic tree of selected WrbA, NAD(P)H:quinone oxidoreductase, and flavodoxin sequences. The full alignment of these sequences is shown in Fig. 1. The scale represents the average number of amino acid substitutions per site. $WrbA_{E.\ coli}$ and $WrbA_{A.\ fulgidus}$ are in bold type. Organisms and ORF designations from the corresponding genomic sequence: *A. fulgidus* WrbA (gi: 11497955), *A. thaliana* FQR1 (gi: 21539481), *B. cepacia* WrbA (gi: 46310790), *C. aurantiacus* WrbA (gi: 53798190), *C. crescentus* WrbA (gi: 13422034), *C. beijerinckii* Fldx (gi: 1941945), *D. gigas* Fldx (gi: 40801), *D. radiodurans* WrbA (gi: 58177611), *Exiguobacterium* sp. strain 255-15 WrbA (gi: 68054352), *E. carotovora* WrbA (gi: 49613050), *E. coli* WrbA (gi: 148264) and Fldx (gi: 145986), *G. trabeum* QR1 (gi: 30027749) and QR2 (gi: 33668045), *M. acetivorans* WrbA (gi: 19915027), *M. avium* WrbA (gi: 41409133), *M. barkeri* WrbA (gi: 31793946), *Mesorhizobium* sp. strain BNC1 WrbA (gi: 68191386), *M. degradans* WrbA (gi: 48860599), *M. mazei* WrbA (gi: 21228326), *N. crassa* WrbA (gi: 38566940), *N. punctiforme* WrbA (gi: 23129682), *P. arcticum* WrbA (gi: 71038102), *P. chrysosporium* QR (gi: 4454993), *Polaromonas* sp. strain JS666 WrbA (gi: 67847813), *P. aeruginosa* WrbA (gi: 9946855), *S. pombe* Obr1 (gi: 2462689), *S. solfataricus* WrbA (gi: 15899861), *S. todakii* WrbA (gi: 15621890), *T. versicolor* QR2 (gi: 12484052), *X. fastidiosa* WrbA (gi: 22993897), *Y. lipolytica* WrbA (gi: 49647887), and *Y. pestis* WrbA (gi: 22126332).

developed at pH 6.6, as indicated by the yellow color of the fractions containing $WrbA_{E.\ coli}$. However, the $WrbA_{E.\ coli}$ protein that eluted from the second Q-Sepharose column developed at pH 7.8 did not contain FMN, indicating that binding of FMN in $WrbA_{E.\ coli}$ is pH dependent. After reconstitution with FMN, a ratio of 1.04 ± 0.03 FMN molecules per monomer was obtained, suggesting 1 FMN molecule per monomer, consistent with a previous report (29). The reconstituted protein exhibited a spectrum characteristic of oxidized flavoproteins (Fig. 4). Other than an initial heat denaturation step, $WrbA_{A.\ fulgidus}$ was purified in the same way as $WrbA_{E.\ coli}$, although $WrbA_{A.\ fulgidus}$ retained FMN through all steps of the purification, with a ratio of 0.87 ± 0.05 FMN molecule per monomer upon elution from the second Q-Sepharose column developed at pH 7.8. After reconstitution, a ratio of 1.10 ± 0.04 FMN molecules per monomer was obtained, suggesting 1 FMN molecule per monomer, and the reconstituted protein exhibited a spectrum characteristic of oxidized flavoproteins. Differences in the UV-visible spectra at the peak centered on 450 nm suggest that the FMN environment is somewhat different in $WrbA_{E.\ coli}$ than in $WrbA_{A.\ fulgidus}$ (Fig. 4). The ratio of absorbance of $WrbA_{E.\ coli}$ at 274 nm/450 nm was 4.7, with an extinction coefficient of $\varepsilon_{450} = 11.6\ mM^{-1}\ cm^{-1}$. The ratio of absorbance of $WrbA_{A.\ fulgidus}$ at 274 nm/457 nm was 3.7, with an extinction coefficient of $\varepsilon_{457} = 14.0\ mM^{-1}\ cm^{-1}$.

Hydrophobicity plots were produced with TMpred (available at ExPASy's Proteomic Tools) to clarify whether WrbA is localized at the membrane. The plots indicated two hydrophobic regions. The first of these overlaps with the flavodoxin signature motif, suggesting that this region binds the flavin and contributes to stabilization of the αβ twisted open-sheet fold typical of flavodoxin-like proteins. The second hydrophobic span, predicted to be a transmembrane region, overlaps the unique additional αβ unit (Fig. 1). Gorman and Shapiro found that this unique hydrophobic region significantly contributes to tetramerization and is located at the core of the tetramer (26). Thus, WrbA proteins do not appear to be integral membrane proteins, although it is unclear whether WrbA proteins are membrane associated.

Since sequence comparisons indicated that $WrbA_{E.\ coli}$ and $WrbA_{A.\ fulgidus}$ are related to fungal and plant NQOs, this activity was determined for both $WrbA_{E.\ coli}$ and $WrbA_{A.\ fulgidus}$. As shown in Table 1, both $WrbA_{E.\ coli}$ and $WrbA_{A.\ fulgidus}$ were able to couple electron transfer from NADH to several quinones. There was significantly less activity with cytochrome *c* (<1%) and no activity with benzyl viologen, methyl viologen (paraquat), FMN, flavin adenine dinucleotide (FAD), F_{420}, 2-hydroxyphenazine, 2-hydroxynaphthoquinone, or 9,10-anthroquinone-2,6-disulfonate (data not shown). The apparent kinetic parameters determined for $WrbA_{E.\ coli}$ or $WrbA_{A.\ fulgidus}$ catalyzing electron transfer from NAD(P)H to 1,4-benzoquinone or to K_3FeCN_6 (Table 2) support the idea that the activities are physiological. Both $WrbA_{E.\ coli}$ and $WrbA_{A.\ fulgidus}$ preferred NADH over NADPH, which suggests that the enzyme does not play a role in biosynthesis since NADPH is the preferred electron donor in biosynthetic pathways of prokaryotes.

The pH dependence of electron transfer from NADH to menadione was measured for both $WrbA_{E.\ coli}$ and $WrbA_{A.\ fulgidus}$ (Fig. 5). Apparent initial velocities showed that $WrbA_{E.\ coli}$ retained nearly 95% activity over a pH range of 6.0 to 8.0 and

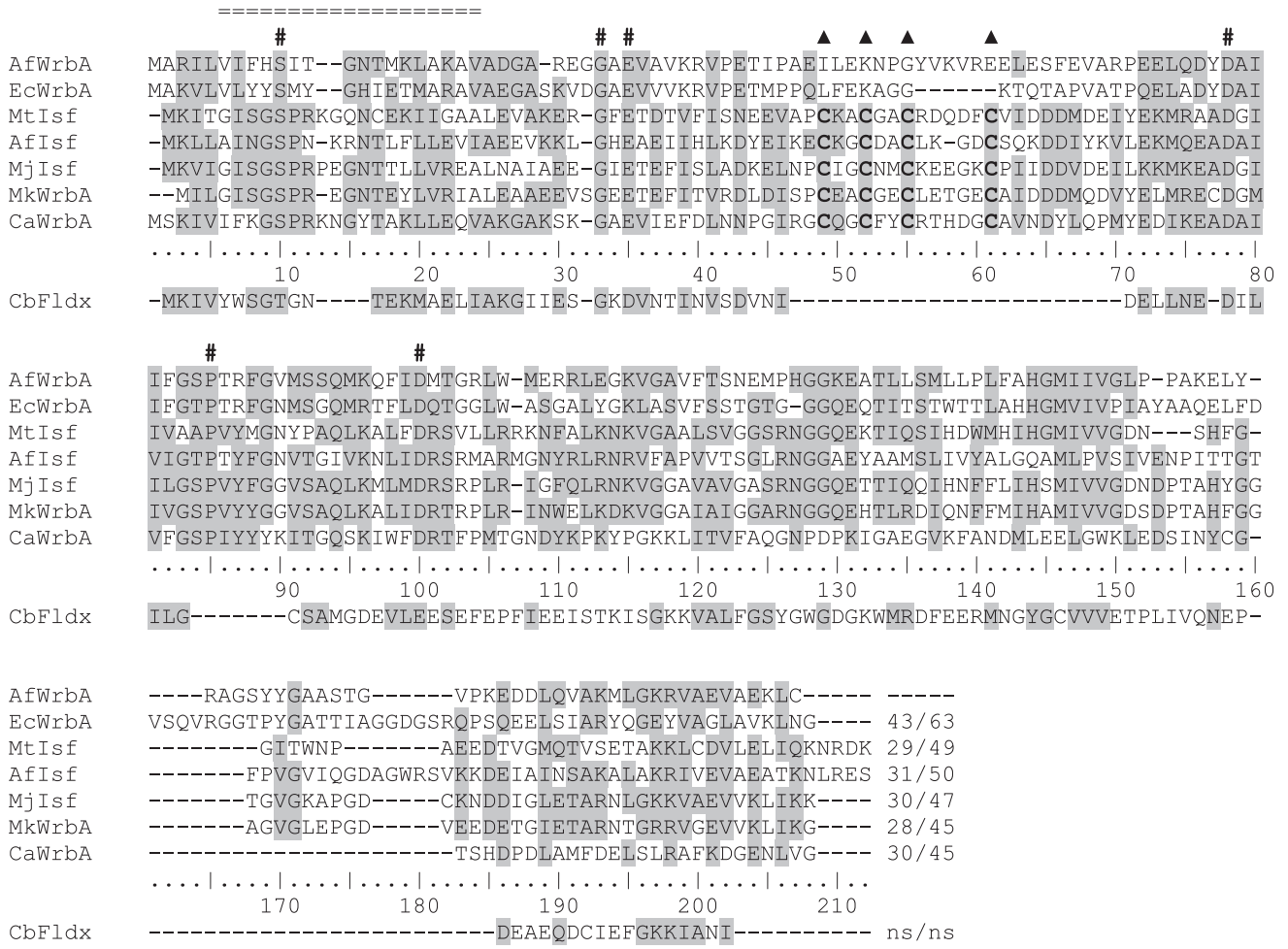

FIG. 3. Sequence alignment with WrbA sequences, Isf sequences, and misannotated WrbA sequences that have a compact cysteine motif. Numerical values at the C terminus indicate percent identity/percent similarity to *E. coli* WrbA. ns, not significant; #, completely conserved residues; = = = = = =, region of the flavodoxin signature motif; ▲, compact cysteine motif. Organisms and ORF designations from the corresponding genomic sequence: *A. fulgidus* Isf (gi: 11499480), *A. fulgidus* WrbA (gi: 11497955), *Clostridium acetotrophicum* WrbA (gi: 15896732), *E. coli* WrbA (gi: 148264), *C. beijerinckii* Fldx (gi: 1941945), *Methanosarcina jannaschii* Isf (gi: 15669271), *Methanopyrus kandleri* WrbA (gi: 20094374), and *M. thermophila* Isf (gi: 2246438).

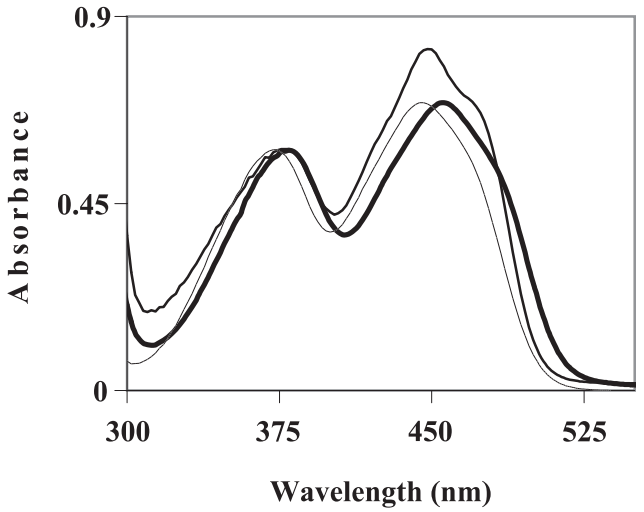

FIG. 4. UV-visible light spectra of reconstituted, oxidized $WrbA_{E.\ coli}$ and $WrbA_{A.\ fulgidus}$. Comparison of WrbA-bound FMN versus free FMN. $WrbA_{A.\ fulgidus}$, —; $WrbA_{E.\ coli}$, —; free FMN, - - -.

$WrbA_{A.\ fulgidus}$ retained at least 95% activity from pH 5.0 to 8.5. The temperature dependence of electron transfer from NADH to menadione was measured for both $WrbA_{E.\ coli}$ and $WrbA_{A.\ fulgidus}$. The apparent initial velocities reflect the optimal growth temperatures of the respective species. In the linear range of highest activity, Arrhenius plots of the apparent initial velocities show that the E_a for $WrbA_{A.\ fulgidus}$ is 3.63

TABLE 1. Specific activities of $WrbA_{E.\ coli}$ and $WrbA_{A.\ fulgidus}$

Electron acceptor	Avg sp act (U^a mg^{-1}) ± SD	
	$WrbA_{E.\ coli}$	$WrbA_{A.\ fulgidus}$
1,4-Benzoquinone	990 ± 30	25,000 ± 850
1,4-Naphthoquinone	560 ± 30	8,900 ± 260
Menadione	430 ± 10	1,300 ± 10
2,3-Dihydroxy-5-methyl-1,4-benzoquinone	930 ± 60	6,700 ± 140
Potassium ferricyanide	50 ± 1.6	1,400 ± 80
Dichloroindolphenol	160 ± 3.0	1,400 ± 70

[a] Micromoles of NADH oxidized per minute.

TABLE 2. Apparent kinetic parameters of $WrbA_{E.\ coli}$ and $WrbA_{A.\ fulgidus}$

Substrate	$WrbA_{E.\ coli}$			$WrbA_{A.\ fulgidus}$		
	k_{cat}^{app}/K_m^{app} (M^{-1} s^{-1})	k_{cat}^{app} (s^{-1})	K_m^{app} (μM)	k_{cat}^{app}/K_m^{app} (M^{-1} s^{-1})	k_{cat}^{app} (s^{-1})	K_m^{app} (μM)
NADH[a]	$6.4 \times 10^5 \pm 0.20 \times 10^5$[c]	8.9 ± 0.064	14 ± 0.43	$6.3 \times 10^6 \pm 0.59 \times 10^6$	120 ± 2.9	19 ± 1.7
NADPH[a]	$3.5 \times 10^4 \pm 0.26 \times 10^4$	6.0 ± 0.15	170 ± 12	$5.5 \times 10^6 \pm 0.33 \times 10^6$	170 ± 2.4	31 ± 1.8
1,4-Benzoquinone[b]	$6.4 \times 10^7 \pm 0.14 \times 10^7$	370 ± 1.7	5.8 ± 0.12	$8.6 \times 10^7 \pm 0.090 \times 10^7$	3,200 ± 130	37 ± 3.6

[a] K_3FeCN_6 was the electron acceptor.
[b] NADH was the electron donor.
[c] Values are averages and standard deviations.

kcal/mol and that for $WrbA_{E.\ coli}$ is 1.88 kcal/mol (Fig. 6). The Arrhenius plots also suggest that the kinetic system undergoes a temperature-dependent shift that increases the activation energy of the rate-limiting steps when the temperature dips below 30°C.

Under aerobic conditions, auto-oxidation took about 20 min for 10 μM reduced $WrbA_{E.\ coli}$ or $WrbA_{A.\ fulgidus}$ (not shown). Despite this low activity with O_2, all activity assays were conducted anaerobically to prohibit electron acceptors from interacting with O_2 to produce ROS, which might affect the rates.

Phenotypic screening at Biolog, Inc. A *wrbA* knockout was constructed from *E. coli* K-12 MG1655, and the knockout and WT strains were submitted to Biolog, Inc., for phenotypic analyses. The growth of the *wrbA* mutant strain was compared to the growth of the WT strain at 37°C in Luria broth with nearly 2,000 phenotypes tested. (Phenotypes tested are available from Biolog, Inc., at http://www.biolog.com/phenoMicro.html.) No phenotypes were gained; however, *N*-trichloromethyl-mercapto-4-cyclohexene-1,2-dicarboximide and 8-hydroxyquinoline significantly inhibited the growth of the *wrbA* knockout relative to the WT, which is consistent with a role for WrbA in protecting against environmental stressors through its quinone reductase activity.

DISCUSSION

$WrbA_{E.\ coli}$ was previously proposed to play a role as an accessory element in blocking TrpR-specific transcriptional processes (66); however, this role has been questioned (29) and the function is unknown. Further, $WrbA_{E.\ coli}$ was the only biochemically characterized member of the WrbA family and no enzyme activity has been reported. Here, we demonstrate that $WrbA_{E.\ coli}$ has NAD(P)H-dependent redox activity and reduces quinones. We also report the characterization of $WrbA_{A.\ fulgidus}$, a homologue from a hyperthermophilic archaeon, and show that it has the same redox activity. Phylogenetic analyses indicate that several characterized fungal and plant NQOs belong to the WrbA family, which suggests that this enzyme activity is a defining characteristic common to the WrbA family. Further, the activities and kinetic constants of $WrbA_{E.\ coli}$ and $WrbA_{A.\ fulgidus}$ reported here correlate well with those reported for NQO homologues in *G. trabeum* (33) and *P. chrysosporium* (11).

At least six other protein families with NQO activity are known, three of which have been designated type I through type III. Other than activity, the WrbA family bears no sequence similarity to and has unique structural characteristics not present in any of the six other protein families; in addition to the unique αβ unit, WrbA has one FMN molecule per monomer and participates in a dimer-tetramer equilibrium. Thus, we adopt the nomenclature initiated by type I through type III and designate the WrbA family type IV. Types I to III are more commonly referred to as NADH dehydrogenases. Perhaps the best-characterized type I protein is NADH-dependent complex I, the H^+/Na^+-transporting integral membrane complex composed of up to 46 subunits that participates in electron transfer in prokaryotes from the *Bacteria* domain during respiration (46, 65). Type II NADH dehydrogenase is usu-

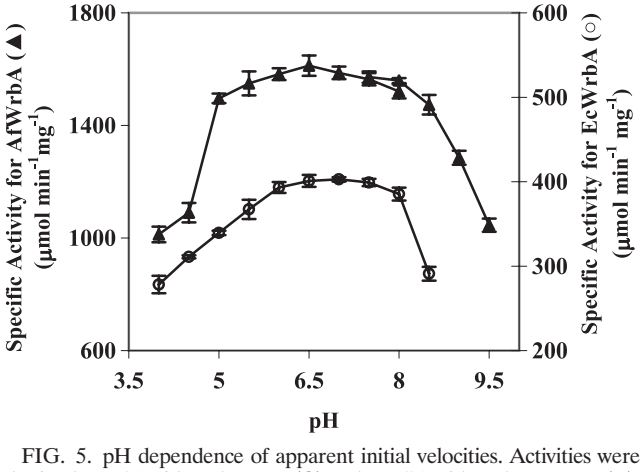

FIG. 5. pH dependence of apparent initial velocities. Activities were obtained at 37°C with $WrbA_{E.\ coli}$ (○) and at 65°C with $WrbA_{A.\ fulgidus}$ (▲).

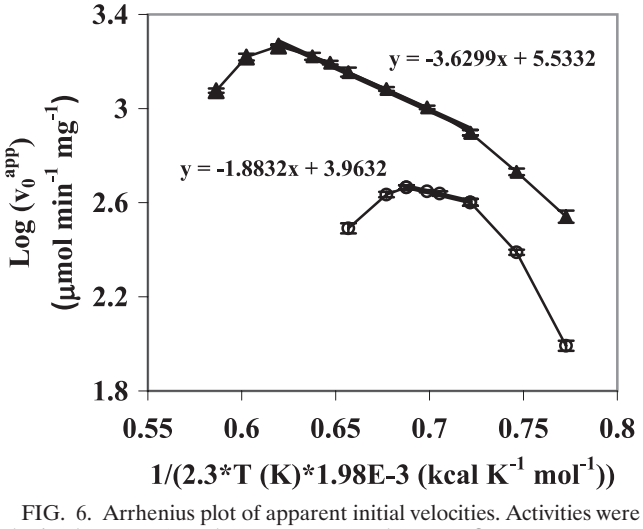

FIG. 6. Arrhenius plot of apparent initial velocities. Activities were obtained at pH 7.2. $WrbA_{A.\ fulgidus}$, ▲; $WrbA_{E.\ coli}$, ○.

ally a single polypeptide and does not generate a chemical gradient (46). The Na^+-transporting (type III) NAD(P)H dehydrogenase is composed of six or seven subunits and is responsible for generating an Na^+ potential that can be used for flagellar movement or for substrate transfer (8, 46). There is no standard nomenclature for the remaining three protein families with NQO activity. The first of these three families is eukaryotic DT-diaphorase–NQO1, a dimeric FAD-containing protein that reduces antitumor quinones with NAD(P)H (15, 57). The second family is FAD-containing NQO2, which has sequence similarity to NQO1, uses dihydronicotinamide riboside as the electron donor, and is resistant to typical inhibitors of DT-diaphorases (15). The third family is ζ-crystalline and is a major protein present in some mammalian ocular lenses which participates in the one-electron reduction of quinones (52).

Possible physiological roles for type IV NQOs. Several NQOs from the *Fungi* and *Viridiplantae* kingdoms identified here as belonging to the WrbA family have been suggested to function in reducing quinones to the hydroquinone state to prevent interaction of the semiquinone with O_2 and production of superoxide. Quinoid compounds are essential to organisms from all domains of life. Quinones are generally tethered to the plasma membrane or freely traverse the lipid bilayer and function in electron transport chains, in cell signaling, and in protection from environmental oxidizers through direct reduction (6, 45). Although they usually serve as electron mediators by cycling between the oxidized (hydroquinone) state and the two-electron reduced (hydroquinol) state, quinones can also participate in deleterious redox cycling through direct interactions with single electron acceptors such as O_2. This one-electron redox cycling leads to the accumulation of reactive oxygen species (ROS) such as superoxide, hydrogen peroxide, and the hydroxyl radical (1, 3, 7, 9–13, 22, 24, 32, 33, 44, 53, 64). Intracellular production of ROS can result in the peroxidation of lipids, the destruction of cofactors, and the hydroxylation of proteins and nucleic acids (1, 16, 21, 23, 24, 40, 55, 63). Several reports suggest that in order to guard against the production of ROS from one-electron redox cycling, a wide diversity of cells have evolved NQOs to maintain quinones in the fully reduced state (1, 10, 11, 15, 30, 32, 33, 42, 47, 54, 58, 64).

A role for the type IV NQO family in alleviating and recovering from oxidative stress through quinone reduction fits the available data, and both $WrbA_{E.\ coli}$ and $WrbA_{A.\ fulgidus}$ derive from organisms that synthesize quinones; *E. coli* synthesizes ubiquinone-8 and menaquinone-8, while *A. fulgidus* produces a menaquinone with a fully saturated heptaprenyl side chain (60). However, NQO activity could also suggest a role in cell signaling, as has been proposed for a type IV NQO found in yeast (*Schizosaccharomyces pombe* Obr1 in Fig. 2) (19, 48, 56, 62). Numerous studies have shown that the redox status of the quinone pool is tightly coupled to cell signaling and cell growth of diverse cell types (4, 27, 36, 49). More specifically, the ArcA-ArcB two-component system of *E. coli*, which regulates cellular transcription in response to external electron acceptors, is one method by which *E. coli* controls expression in response to redox changes (25, 43). As previously reported, *E. coli wrbA* is repressed by phosphorylated ArcA, which is phosphorylated when the quinone pool is reduced (41). Further, WrbA is upregulated when *E. coli* enters the stationary phase and in the presence of a variety of stressors, such as acids, salts, H_2O_2, and diauxie, under the control of RpoS (the stress response sigma factor, σ^s or σ^{38}) (14, 17, 31, 35, 50, 51, 59, 61). Another study demonstrated that, under anaerobic conditions, *E. coli wrbA* is also repressed by fumarate and nitrate reductase regulatory protein, suggesting that $WrbA_{E.\ coli}$ does not function during anaerobiosis (34). Cumulatively, these expression studies suggest that $WrbA_{E.\ coli}$ functions in response to environmental stress when various electron transfer chains are affected or when the environment is highly oxidizing. Although the idea is speculative, $WrbA_{E.\ coli}$ could function in cell signaling by reducing the quinone pool, which would subsequently signal redox sensors such as the ArcA modulon. Chang and coworkers speculated about a similar mechanism for an ζ-crystalline type of NQO that is expressed under stress and reduces the quinone pool, ultimately phosphorylating ArcA and inducing a shift from respiratory metabolism to fermentative metabolism (14).

ACKNOWLEDGMENTS

This work was supported by DOE grant DE-FG02-95ER20198, by a grant from the NASA Astrobiology Institute, and in part by a grant from the Integrative Biosciences Program at The Pennsylvania State University.

We thank Sarah Ades, Tracy Nixon, and Ming Tien for valuable direction, discussion, and support.

REFERENCES

1. **Adams, M. A., and Z. Jia.** 2005. Structural and biochemical evidence for an enzymatic quinone redox cycle in *Escherichia coli*: identification of a novel quinol monooxygenase. J. Biol. Chem. **280:**8358–8363.
2. **Andrade, S. L., F. Cruz, C. L. Drennan, V. Ramakrishnan, D. C. Rees, J. G. Ferry, and O. Einsle.** 2005. Structures of the iron-sulfur flavoproteins from *Methanosarcina thermophila* and *Archaeoglobus fulgidus*. J. Bacteriol. **187:** 3848–3854.
3. **Arroyo, A., F. Navarro, C. Gomez-Diaz, F. Crane, F. Alcain, P. Navas, and J. Villalba.** 2000. Interactions between ascorbyl free radical and coenzyme Q at the plasma membrane. J. Bioenerg. Biomembr. **32:**199–210.
4. **Bauer, C. E., S. Elsen, and T. H. Bird.** 1999. Mechanisms for redox control of gene expression. Annu. Rev. Microbiol. **53:**495–523.
5. **Becker, D. F., U. Leartsakulpanich, K. K. Surerus, J. G. Ferry, and S. W. Ragsdale.** 1998. Electrochemical and spectroscopic properties of the iron-sulfur flavoprotein from *Methanosarcina thermophila*. J. Biol. Chem. **273:** 26462–26469.
6. **Berry, S.** 2002. The chemical basis of membrane bioenergetics. J. Mol. Evol **54:**595–613.
7. **Boersma, M. G., W. G. Balvers, S. Boeren, J. Vervoort, and I. M. Rietjens.** 1994. NADPH-cytochrome reductase catalysed redox cycling of 1,4-benzoquinone; hampered at physiological conditions, initiated at increased pH values. Biochem. Pharmacol. **47:**1949–1955.
8. **Bogachev, A. V., and M. I. Verkhovsky.** 2005. Na^+-translocating NADH: quinone oxidoreductase: progress achieved and prospects of investigations. Biochemistry (Moscow) **70:**143–149.
9. **Bond, D. R., and D. R. Lovley.** 2002. Reduction of Fe(III) oxide by methanogens in the presence and absence of extracellular quinones. Environ. Microbiol. **4:**115–124.
10. **Brock, B. J.** 1995. Purification and characterization of a 1,4-benzoquinone reductase from the basidiomycete *Phanerochaete chrysosporium*. Appl. Environ. Microbiol. **61:**3076–3081.
11. **Brock, B. J., and M. H. Gold.** 1996. 1,4-Benzoquinone reductase from basidiomycete *Phanerochaete chrysosporium*: spectral and kinetic analysis. Arch. Biochem. Biophys. **331:**31–40.
12. **Cervantes, F., S. van der Velde, G. Lettinga, and J. Field.** 2000. Quinones as terminal electron acceptors for anaerobic microbial oxidation of phenolic compounds. Biodegradation **11:**313–321.
13. **Cervantes, F. J., F. A. de Bok, T. Duong-Dac, A. J. Stams, G. Lettinga, and J. A. Field.** 2002. Reduction of humic substances by halorespiring, sulphate-reducing and methanogenic microorganisms. Environ. Microbiol. **4:**51–57.
14. **Chang, D. E., D. J. Smalley, and T. Conway.** 2002. Gene expression profiling of *Escherichia coli* growth transitions: an expanded stringent response model. Mol. Microbiol. **45:**289–306.
15. **Chen, S., K. Wu, and R. Knox.** 2000. Structure-function studies of DT-diaphorase (NQO1) and NRH: quinone oxidoreductase (NQO2). Free Radic. Biol. Med. **29:**276–284.

16. **Chen, S. X., and P. Schopfer.** 1999. Hydroxyl-radical production in physiological reactions. A novel function of peroxidase. Eur. J. Biochem. **260:**726–735.
17. **Cheung, K. J., V. Badarinarayana, D. W. Selinger, D. Janse, and G. M. Church.** 2003. A microarray-based antibiotic screen identifies a regulatory role for supercoiling in the osmotic stress response of *Escherichia coli*. Genome Res. **13:**206–215.
18. **Cohen, R., M. R. Suzuki, and K. E. Hammel.** 2004. Differential stress-induced regulation of two quinone reductases in the brown rot basidiomycete *Gloeophyllum trabeum*. Appl. Environ. Microbiol. **70:**324–331.
19. **Daher, B. S., E. J. Venancio, S. M. de Freitas, S. N. Bao, P. V. Vianney, R. V. Andrade, A. S. Dantas, C. M. Soares, I. Silva-Pereira, and M. S. Felipe.** 2005. The highly expressed yeast gene *pby20* from *Paracoccidioides brasiliensis* encodes a flavodoxin-like protein. Fungal Genet. Biol. **42:**434–443.
20. **Datsenko, K. A., and B. L. Wanner.** 2000. One-step inactivation of chromosomal genes in *Escherichia coli* K-12 using PCR products. Proc. Natl. Acad. Sci. USA **97:**6640–6645.
21. **Fang, Y. Z., S. Yang, and G. Wu.** 2002. Free radicals, antioxidants, and nutrition. Nutrition **18:**872–879.
22. **Finneran, K. T., H. M. Forbush, C. V. VanPraagh, and D. R. Lovley.** 2002. *Desulfitobacterium metallireducens* sp. nov., an anaerobic bacterium that couples growth to the reduction of metals and humic acids as well as chlorinated compounds. Int. J. Syst. Evol. Microbiol. **52:**1929–1935.
23. **Fridovich, I.** 1998. Oxygen toxicity: a radical explanation. J. Exp. Biol. **201**(Pt. 8)**:**1203–1209.
24. **Fridovich, I.** 1997. Superoxide anion radical (O_2^-), superoxide dismutases, and related matters. J. Biol. Chem. **272:**18515–18517.
25. **Georgellis, D., O. Kwon, and E. C. Lin.** 2001. Quinones as the redox signal for the arc two-component system of bacteria. Science **292:**2314–2316.
26. **Gorman, J., and L. Shapiro.** 2005. Crystal structures of the tryptophan repressor binding protein WrbA and complexes with flavin mononucleotide. Protein Sci. **14:**3004–3012.
27. **Grabbe, R., and R. A. Schmitz.** 2003. Oxygen control of *nif* gene expression in *Klebsiella pneumoniae* depends on NifL reduction at the cytoplasmic membrane by electrons derived from the reduced quinone pool. Eur. J. Biochem. **270:**1555–1566.
28. **Grandori, R., and J. Carey.** 1994. Six new candidate members of the α/β twisted open-sheet family detected by sequence similarity to flavodoxin. Protein Sci. **3:**2185–2193.
29. **Grandori, R., P. Khalifah, J. A. Boice, R. Fairman, K. Giovanielli, and J. Carey.** 1998. Biochemical characterization of WrbA, founding member of a new family of multimeric flavodoxin-like proteins. J. Biol. Chem. **273:** 20960–20966.
30. **Hayashi, M., K. Hasegawa, Y. Oguni, and T. Unemoto.** 1990. Characterization of FMN-dependent NADH-quinone reductase induced by menadione in *Escherichia coli*. Biochim. Biophys. Acta **1035:**230–236.
31. **Ishihama, A.** 2000. Functional Modulation of *Escherichia coli* RNA polymerase. Annu. Rev. Microbiol. **54:**499–518.
32. **Jaiswal, A. K.** 2000. Regulation of genes encoding NAD(P)H: quinone oxidoreductases. Free Radic. Biol. Med. **29:**254–262.
33. **Jensen, K. A., Jr., Z. C. Ryan, A. Vanden Wymelenberg, D. Cullen, and K. E. Hammel.** 2002. An NADH:quinone oxidoreductase active during biodegradation by the brown-rot basidiomycete *Gloeophyllum trabeum*. Appl. Environ. Microbiol. **68:**2699–2703.
34. **Kang, Y., K. D. Weber, Y. Qiu, P. J. Kiley, and F. R. Blattner.** 2005. Genome-wide expression analysis indicates that FNR of *Escherichia coli* K-12 regulates a large number of genes of unknown function. J. Bacteriol. **187:**1135–1160.
35. **Kirkpatrick, C., L. M. Maurer, N. E. Oyelakin, Y. N. Yoncheva, R. Maurer, and J. L. Slonczewski.** 2001. Acetate and formate stress: opposite responses in the proteome of *Escherichia coli*. J. Bacteriol. **183:**6466–6477.
36. **Kowaltowski, A. J., R. F. Castilho, and A. E. Vercesi.** 2001. Mitochondrial permeability transition and oxidative stress. FEBS Lett. **495:**12–15.
37. **Laskowski, M. J., K. A. Dreher, M. A. Gehring, S. Abel, A. L. Gensler, and I. M. Sussex.** 2002. FQR1, a novel primary auxin-response gene, encodes a flavin mononucleotide-binding quinone reductase. Plant Physiol. **128:**578–590.
38. **Latimer, M. T., M. H. Painter, and J. G. Ferry.** 1996. Characterization of an iron-sulfur flavoprotein from *Methanosarcina thermophila*. J. Biol. Chem. **271:**24023–24028.
39. **Leartsakulpanich, U., M. L. Antonkine, and J. G. Ferry.** 2000. Site-specific mutational analysis of a novel cysteine motif proposed to ligate the 4Fe-4S cluster in the iron-sulfur flavoprotein of the thermophilic methanoarchaeon *Methanosarcina thermophila*. J. Bacteriol. **182:**5309–5316.
40. **Lim, P., G. E. Wuenschell, V. Holland, D. H. Lee, G. P. Pfeifer, H. Rodriguez, and J. Termini.** 2004. Peroxyl radical mediated oxidative DNA base damage: implications for lipid peroxidation induced mutagenesis. Biochemistry **43:** 15339–15348.
41. **Liu, X., and P. De Wulf.** 2004. Probing the ArcA-P modulon of *Escherichia coli* by whole genome transcriptional analysis and sequence recognition profiling. J. Biol. Chem. **279:**12588–12597.
42. **Long, D. J., II, and A. K. Jaiswal.** 2000. NRH:quinone oxidoreductase 2 (NQO2). Chem. Biol. Interact. **129:**99–112.
43. **Malpica, R., B. Franco, C. Rodriguez, O. Kwon, and D. Georgellis.** 2004. Identification of a quinone-sensitive redox switch in the ArcB sensor kinase. Proc. Natl. Acad. Sci. USA **101:**13318–13323.
44. **Matvienko, M., A. Wojtowicz, R. Wrobel, D. Jamison, Y. Goldwasser, and J. I. Yoder.** 2001. Quinone oxidoreductase message levels are differentially regulated in parasitic and non-parasitic plants exposed to allelopathic quinones. Plant J. **25:**375–387.
45. **Meganathan, R.** 2001. Ubiquinone biosynthesis in microorganisms. FEMS Microbiol. Lett. **203:**131–139.
46. **Melo, A. M., T. M. Bandeiras, and M. Teixeira.** 2004. New insights into type II NAD(P)H:quinone oxidoreductases. Microbiol. Mol. Biol. Rev. **68:**603–616.
47. **Morre, D. J.** 2004. Quinone oxidoreductases of the plasma membrane. Methods Enzymol. **378:**179–199.
48. **Naresh, A., S. Saini, and J. Singh.** 2003. Identification of Uhp1, a ubiquitinated histone-like protein, as a target/mediator of Rhp6 in mating-type silencing in fission yeast. J. Biol. Chem. **278:**9185–9194.
49. **Oh, J. I., and S. Kaplan.** 2000. Redox signaling: globalization of gene expression. EMBO J. **19:**4237–4247.
50. **Phadtare, S., I. Kato, and M. Inouye.** 2002. DNA microarray analysis of the expression profile of *Escherichia coli* in response to treatment with 4,5-dihydroxy-2-cyclopenten-1-one. J. Bacteriol. **184:**6725–6729.
51. **Pomposiello, P. J., M. H. Bennik, and B. Demple.** 2001. Genome-wide transcriptional profiling of the *Escherichia coli* responses to superoxide stress and sodium salicylate. J. Bacteriol. **183:**3890–3902.
52. **Rao, P. V., C. M. Krishna, and J. S. Zigler, Jr.** 1992. Identification and characterization of the enzymatic activity of zeta-crystallin from guinea pig lens. A novel NADPH:quinone oxidoreductase. J. Biol. Chem. **267:**96–102.
53. **Roginsky, V., T. Barsukova, G. Bruchelt, and H. Stegmann.** 1998. Kinetics of redox interaction between substituted 1,4-benzoquinones and ascorbate under aerobic conditions: critical phenomena. Free Radic. Res. **29:**115–125.
54. **Ross, D., J. K. Kepa, S. L. Winski, H. D. Beall, A. Anwar, and D. Siegel.** 2000. NAD(P)H:quinone oxidoreductase 1 (NQO1): chemoprotection, bioactivation, gene regulation and genetic polymorphisms. Chem. Biol. Interact. **129:** 77–97.
55. **Schopfer, P., A. Liszkay, M. Bechtold, G. Frahry, and A. Wagner.** 2002. Evidence that hydroxyl radicals mediate auxin-induced extension growth. Planta **214:**821–828.
56. **Shimanuki, M., Y. Saka, M. Yanagida, and T. Toda.** 1995. A novel essential fission yeast gene *pad1*$^+$ positively regulates *pap1*$^+$-dependent transcription and is implicated in the maintenance of chromosome structure. J. Cell Sci. **108:**569–579.
57. **Siegel, D., D. L. Gustafson, D. L. Dehn, J. Y. Han, P. Boonchoong, L. J. Berliner, and D. Ross.** 2004. NAD(P)H:quinone oxidoreductase 1: role as a superoxide scavenger. Mol. Pharmacol. **65:**1238–1247.
58. **Sparla, F., G. Tedeschi, P. Pupillo, and P. Trost.** 1999. Cloning and heterologous expression of NAD(P)H:quinone reductase of *Arabidopsis thaliana*, a functional homologue of animal DT-diaphorase. FEBS Lett. **463:**382–386.
59. **Tao, H., C. Bausch, C. Richmond, F. R. Blattner, and T. Conway.** 1999. Functional genomics: expression analysis of *Escherichia coli* growing on minimal and rich media. J. Bacteriol. **181:**6425–6440.
60. **Tindall, B., K. Stetter, and M. Collins.** 1989. A novel, fully saturated menaquinone from the thermophilic, sulphate-reducing archaebacterium *Archaeoglobus fulgidus*. J. Gen. Microbiol. **135:**693–696.
61. **Tucker, D. L., N. Tucker, and T. Conway.** 2002. Gene expression profiling of the pH response in *Escherichia coli*. J. Bacteriol. **184:**6551–6558.
62. **Turi, T. G., P. Webster, and J. K. Rose.** 1994. Brefeldin A sensitivity and resistance in *Schizosaccharomyces pombe*. Isolation of multiple genes conferring resistance. J. Biol. Chem. **269:**24229–24236.
63. **Vranova, E., D. Inze, and F. Van Breusegem.** 2002. Signal transduction during oxidative stress. J. Exp. Bot. **53:**1227–1236.
64. **Wrobel, R. L.** 2002. Heterologous expression and biochemical characterization of an NAD(P)H: quinone oxidoreductase from the hemiparasitic plant *Triphysaria versicolor*. Plant Physiol. Biochem. **40:**265–272.
65. **Yagi, T., and A. Matsuno-Yagi.** 2003. The proton-translocating NADH-quinone oxidoreductase in the respiratory chain: the secret unlocked. Biochemistry **42:**2266–2274.
66. **Yang, W., L. Ni, and R. Somerville.** 1993. A stationary-phase protein of *Escherichia coli* that affects the mode of association between the *trp* repressor protein and operator-bearing DNA. Proc. Natl. Acad. Sci. USA **90:**5796–5800.
67. **Zhao, T., F. Cruz, and J. G. Ferry.** 2001. Iron-sulfur flavoprotein (Isf) from *Methanosarcina thermophila* is the prototype of a widely distributed family. J. Bacteriol. **183:**6225–6233.